Tunable the buffer layers of solution processed inverted P3HT:PC61BM solar cell

Conference Paper · January 2024

DOI: 10.1063/5.0178042

3 authors:

Amba Sankar
Institute for Plasma Research
11 PUBLICATIONS **148** CITATIONS
SEE PROFILE

Nanda Kumar
PSG College of Arts and Science
10 PUBLICATIONS **39** CITATIONS
SEE PROFILE

Kallol Mohanta
PSG Institute of Advanced Studies
54 PUBLICATIONS **767** CITATIONS
SEE PROFILE

RESEARCH ARTICLE | JANUARY 12 2024

Tunable the buffer layers of solution processed inverted P3HT:$PC_{61}BM$ solar cell

K. N. Amba Sankar; P. Nandakumar ✉; Kallol Mohanta

AIP Conf. Proc. 2995, 020150 (2024)
https://doi.org/10.1063/5.0178042

Tunable the Buffer Layers of Solution processed Inverted P3HT:$PC_{61}BM$ Solar Cell

K. N. Amba Sankar[1], P. Nandakumar[1, a)] and Kallol Mohanta[2,]

[1]*Department of Electronics, PSG College of Arts and Science, Coimbatore-641014, India*
[2]*PSG Institute of Advanced Studies, Coimbatore-641004 Tamil Nadu, India.*

[a)]Corresponding author: nandacjb@gmail.com

Abstract. The present work, we examined the effect of anode interfacial layer molybdenum oxides (MoO_x) with three different rpm on device fabrication of inverted bulk heterojunction (BHJ) solar cell based on a blend of poly (3-hexylthiophene): (6,6) -phenyl C_{61} butyric acid methyl ester (P3HT: $PC_{61}BM$) active layer, zinc oxide (ZnO) as electron transport layer (ETL) and MoOx as hole transport layer (HTL). Buffer layer rpm is one of the important role plays was explored to improve the photovoltaic performance in this device. We found the optimum rpm for MoO_x layer formation and observed with the effect of ZnO-GO/RGO/NG/CQDs composites cathode buffer layer to enhance the performance. Power conversion efficiency was carried out under simulated AM 1.5G illumination of 100 mW/cm^2.

INTRODUCTION

The current life is depends on high energy conception due to our modern life and the energy demand increasing day by day. Resolving this energy deficit, the research has been focused on energy generation from solar cell through photovoltaic effect, which can yield energy directly from sunlight. The BHJ organic photovoltaic have attracted and significant attention due to cost effective, flexible, lightweight and simple device fabrication process[1-4]. The active layer of these BHJ-PSCs is composed by P3HT : PCBM which having massive interface region between electron donor and electron acceptor and the power conversion efficiency (PCE) has reached ~ 6% through optimization of layers morphology, device structure manner and buffer layers interface control[1, 5]. Inverted polymer solar cell having high stability than conventional type PSCs[6] and the most important point is optimization of buffer layers between electrodes and active layers with suitable work-function. ZnO, Ca, TiO2 and reduced graphene oxide (RGO) are utilized as electron transport layer (ETL) coated on ITO substrates and poly (3,4-ethylene dioxy thiophene):poly(styrene sulfonic acid) (PEDOT:PSS), V_2O_5 and MoO_3 these are make use of efficient hole collecting electrode (HTL) coated on the active layer. PEDOT:PSS frequently used in the broad area of organic semiconductor applications. In conventional type PSCs typically used PEDOT:PSS an HTL. But it have strong acidic in nature due to PSS chain to corrodes the hole collecting ITO electrode leads, it reflects degrade the stability and performance of the cells[7].

In this work, we will focus on the impact of rpm on formation of anode buffer layer coating in iPSCs. The MoOx layer coated with three different rpm 5000, 5500 and 6000 and compares the device performance. To enhance the stability and avoid corrosion on ITO we replace PEDOT:PSS and utilized MoO_x as hole transport layer, also we compared ZnO with different composites as electron transport layer and active layer the blend of P3HT:PCBM, indium tin oxide (ITO) and is the electron collecting electrode and aluminum (Al) as a hole collecting electrode.

66th DAE Solid State Physics Symposium
AIP Conf. Proc. 2995, 020150-1–020150-4; https://doi.org/10.1063/5.0178042
Published by AIP Publishing. 978-0-7354-4764-6/$30.00

EXPERIMENT

Preparation of ZnO nanoparticles

The chemical synthesis process of ZnO nanoparticles was as follows[8]: The obtained ZnO nanoparticles were dried at room temperature. ZnO were dissolved in 2-methoxyethanol with the concentration of 20mg/ml. graphene oxide (GO), reduced graphene oxide (RGO),ball milled graphite nanoparticles (MG) and carbon quantum dots (CQD) were dispersed in ethanol with concentration of 0.2mg in 1 ml and 50µl dispersed solution mix with ZnO solution. GO, RGO, MG and CQD were dispersed in ethanol with concentration of 0.2mg in 1 ml and 50µl dispersed solution mix with ZnO solution.

Preparation of MoOx nanoparticles

Low temperature solution processed as follows[9, 10]. The precursor solution was obtained by dissolving 3 g of MoO_3 mix with 20 ml of 30% hydrogen peroxide (H_2O_2) in reflux setup at 80 °C for 2h. The MoO_3 powder was dissolved completely and a clear yellow solution was obtained. The chemical reaction which takes place can be written as

$$MoO_3 + 4\ H_2O_2 = (MoOH)_6 + H_2O + O_2$$

The volume ratio of the MoO3 source to the EG and 2-methoxyethanol was1:0.25:1. After adding ethylene glycol to promote its homogeneity and viscosity and 2-methoxyethanol to cause a reduction/hydrogenation reaction, the solution which now turned blue, was further refluxed at 90°C and 70 °C for 1h and then cool to room temperature for 24h, dried under vacuum chamber at 120 °C for 5h. Finally the MoOx powder dissolved in IPA. GO, RGO, MG and CQDs was synthesized in previous studies[11-14].

Device Fabrication

The photovoltaic device was made-up on ITO-coated glass. The ITO substrates were cleaned through Radio Corporation of America (RCA) cleaning procedure[4, 15]. Then the substrates were dried at 80 °C for 30 min at hot air oven and then UV treated for 30 min to remove remaining organic elements. The n-type buffer layer ZnO composites were coated on patterned substrates with 3000 rpm for 60s and then heat treated at 70 °C in air for 10 min. The active layer was coated in glove box from the blend solution P3HT: PCBM (1:1 weight ratio) in 1,2 dichlorobenzene with 10mg /ml concentration. The concentration of solution was coated at 2000 rpm for 30s to obtain the active layer. The coated substrate was kept at 80°C for 10 min to evaporate residual solvent. The hole transport layer MoOx was coated at 5000, 5500 and 6000 rpm for 40 sec named device (i), device (ii) and device (iii) respectively. Finally Al deposited through a shadow mask under 8×10^{-6} Torr by thermal evaporation. We studied also ZnO composites used as a ETL in PSCs, in device were fabricated with different ETL ZnO composites GO, RGO, MG and CQD v/v % ratio on ZnO solution. GO, RGO, MG and CQD were dispersed in ethanol with concentration of 0.2mg in 1 ml and 50µl dispersed solution mix with ZnO solution named device ZnO/GO, ZnO/RGO, ZnO/MG and ZnO/CQD. All the layers were coated by using spin coating technique.

RESULTS AND DISCUSSION

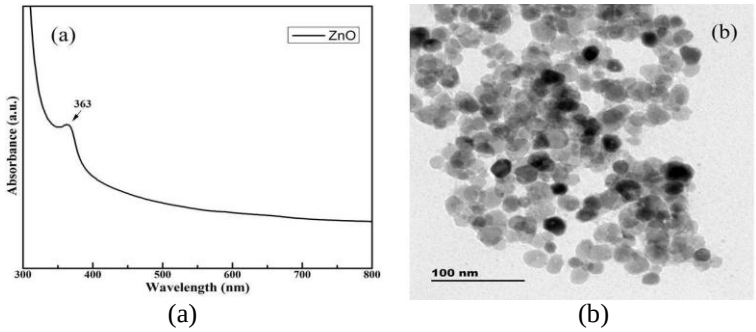

(a) (b)

FIGURE 1. (a) UV – vis absorption spectra of ZnO nanoparticles, (b) TEM image of ZnO nanoparticles.

From fig.1 (a) the UV- vis absorption peak present at 363 nm confirms ZnO nanoparticles[16]. From fig. 1 (b), we can clearly observed from TEM image, we get uniform sphere shape with good crystalline of ZnO nanoparticles.

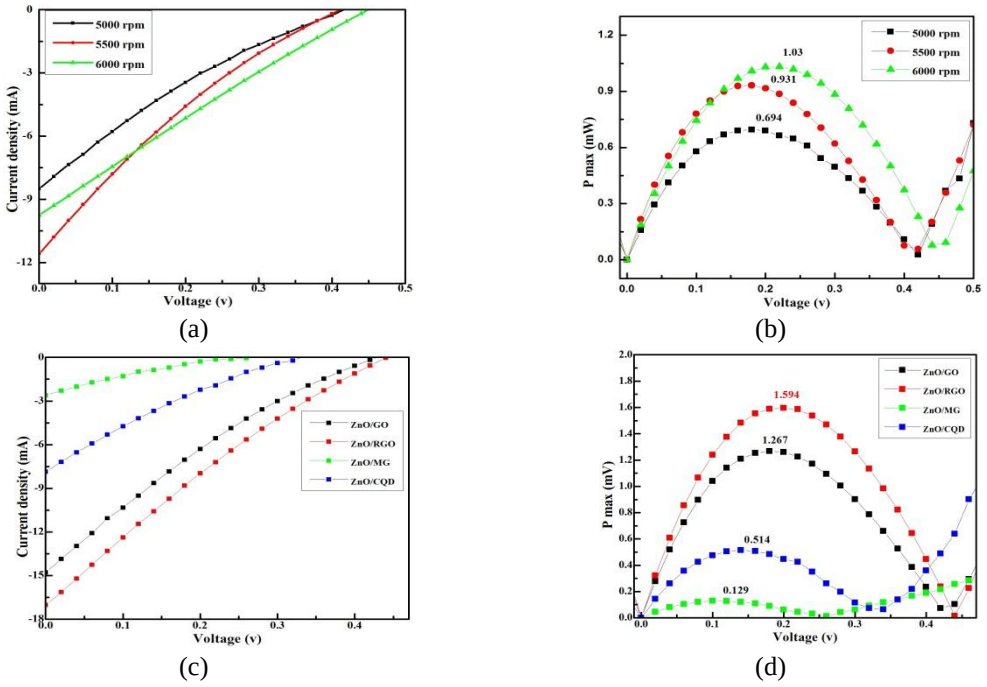

FIGURE 2. (a&c). The J –V characteristics of the iPSCs and Fig. 2 (b&d) showed Power V_s Voltage characteristics of the iPSCs.

Fig. 2 (a&c) illustrates, the J –V characteristics of the ITO/ZnO/P3HT:PCBM/MoOx/Al solar cells device were fabricated with three different 5000, 5500 and 6000 rpm of MoOx layer and constant HTL 6000 rpm with ETL ZnO with different composites. Fig.2 (b&d) illustrates the maximum power point (Pmax) obtained from devices, under simulated solar irradiation of AM 1.5G normalized 100 mW/cm^2.

Photovoltaic Devices Performance

TABLE 1. Details of photovoltaic performance as follows, short circuit current density (Jsc), (open circuit voltage (Voc), fill factor (FF), and efficiency (η). These values were extracted from J-V curves fig. 3 a&c.

Device	MoOx	Voc (V)	Jsc (mA/cm^2)	FF (%)	Pmax (w)	PCE η (%)
(i)	5000 rpm	0.42	-8.49855	19.46797	0.694	0.694
(ii)	5500 rpm	0.42	-11.59209	19.13916	0.931	0.931
(iii)	6000 rpm	0.46	-9.75248	22.9754	1.03	1.03
ZnO/GO	6000 rpm	0.44	-14.78066	19.49482	1.267	1.267
ZnO/RGO	6000 rpm	0.46	-17.02276	20.3633	1.594	1.594
ZnO/MG	6000 rpm	0.28	-2.61764	17.65603	0.129	0.129
ZnO/CQD	6000 rpm	0.34	-7.85818	19.26099	0.514	0.514

TABLE 1. summarized the properties of six photovoltaic samples devices. The iPSCs characteristics of MoO_x layer with different rpm are represented in Fig. 2 a&b. The device (i) 5000 rpm showed a JSC value of -8.49855 mA/cm^2 and device (iii) 6000 rpm showed a Jsc value of -9.75248 mA/cm^2. Depends on variation of spin coating rpm the MoO_x layer thickness would vary and high rpm we reduced the thickness of HTL layer. It enhances the performance of device, increase charge transfer and reduce the interfacial resistance and reducing charge recombination. In ZnO composites ZnO/RGO device get the highest Jsc value -17.02276 mA/cm^2.

CONCLUSION

Solution processed ZnO with composites (ETL) and MoOx (HTL) were used as buffer layers in inverted organic BHJ photovoltaic devices. Device (C) MoOx 6000 rpm get high efficiency value η = 1.03. and ZnO composites ZnO/RGO cell efficiency obtained high. The interaction between the RGO and the ZnO makes fast electron transfer and this composite work well as the (ETL) in photovoltaic devices. In ITO/ZnO:RGO/P3HT:PCBM/MoOx/Al structure of photovoltaic device, a maximum power-conversion efficiency of 1.59 % was obtained.

ACKNOWLEDGMENTS

The authors acknowledge PSG institutions for helping in doing this research work

REFERENCES

1. Burak Kadem, Aseel Hassan, and Wayne Cranton, J. Mater. Sci. Mater. 27, no. 7 (2016): 7038-7048.
2. PanFeng Gao, LiYong Wang, HaiYan Fu, and Yuan Dai, Eur. Polym. J. 172 (2022): 111189.
3. Farah Liyana Khairulaman, Chi Chin Yap, and Mohammad Hafizuddin Hj Jumali, Mater. 283 (2021): 128827.
4. Riccardo Po, Chiara Carbonera, Andrea Bernardi, and Nadia Camaioni, Energy Environ. Sci. 4, no. 2 (2011): 285-310.
5. M. Suresh Kumar, and K. Balachander, Optik, 127, no. 5 (2016): 2725-2731.
6. Yong-Jin Noh, Seok-In Na, and Seok-Soon Kim, Sol. Energy Mater Sol. Cells, 117 (2013): 139-144.
7. Joseph Cameron, and Peter J. Skabara, Mater. Horiz. 7, no. 7 (2020): 1759-1772.
8. Aung Ko Ko Kyaw, Dong Hwan Wang, David Wynands, Jie Zhang, Thuc-Quyen Nguyen, Guillermo C. Bazan, and Alan J. Heeger, Nano Lett. 13, no. 8 (2013): 3796-3801.
9. Anastasia Soultati , Antonios M. Douvas , Dimitra G. Georgiadou , Leonidas C. Palilis, Thomas Bein , Johann M. Feckl, Spyros Gardelis, Mihalis Fakis, Stella Kennou, Polycarpos Falaras, Thomas Stergiopoulos, Nikolaos A. Stathopoulos, Dimitris Davazoglou, Panagiotis Argitis, and Maria Vasilopoulou, Adv. Energy Mater. 4, no. 3 (2014): 1300896.
10. Fengxian Xie, Wallace C.H. Choy, Chuandao Wang, Xinchen Li, Shaoqing Zhang, and Jianhui Hou, Advanced Materials, 25, no. 14 (2013): 2051-2055.
11. Amba Sankar K.N, Lopamudra Bhattacharjee, Sanjeev K. Jat, Rama R. Bhattacharjee, and Kallol Mohanta, ChemistrySelect 2, no. 15 (2017): 4241-4247.
12. K.N. Amba Sankar, C. Sathish Kumar, and Kallol Mohanta, Materials Today: Proceedings 18 (2019): 759-764.
13. K.N. Amba Sankar , P. Nandakumar1, C. Sathishkumar, R. Deepa and Kallol Mohanta, Rasayan J. Chem 14, no. 4 (2021): 2196-2201.
14. P. Nandakumar, K. N. Amba Sankar, A. Shankar Ganesh, BA. Anandh and R. Deepa, Orient. J. Chem., 38, 604-609, (2022).
15. S. Besbes, H. Ben Ouada, Joël Davenas, Laurence Ponsonnet, N. Jaffrezic, and P. Alcouffe, Mater. Sci. Eng. C. 26, no. 2-3 (2006): 505-510.
16. Jagpreet Singh, Sukhmeen Kaur, Gaganpreet Kaur, Soumen Basu, and Mohit Rawat, Green Process. Synth. 8, no. 1 (2019): 272-280.